Biophysical Chemistry 26 (1987) 207–216
Elsevier

BPC 01139

Electro-optical analysis of 'curved' DNA fragments

Stephan Diekmann and Dietmar Pörschke

Max-Planck-Institut für biophysikalische Chemie, 3400 Göttingen, F.R.G.

Accepted 27 February 1987

kinetoplast DNA; Rotational relaxation time; Electric dichroism; curved DNA

The structure of some 'short' DNA fragments with 106–108 base-pairs and of a 'long' kinetoplast DNA fragment with 419 base-pairs has been analyzed by electro-optical procedures. According to their electrophoretic mobilities and circularization probabilities, it was concluded that two of our short fragments with clusters of four and five and six adenosines phased at the period of the double helix are inherently curved with an approximate curvature around 200°. The dichroism decay curves of our short fragments exhibited two processes. A fast one with time constants of approx. 100 ns is attributed to bending; the bending amplitudes observed for the fragments with dA_4 and $dA_{5/6}$ clusters are slightly higher (23 and 29%, respectively) than those observed for control fragments (17–20%). The second process reflects the overall rotational diffusion of the whole fragments and shows some variation with the DNA sequence, but on average the rotation of fragments with dA_4 and $dA_{5/6}$ clusters corresponds to that observed for standard DNA. Since the rotational diffusion coefficients are very strongly dependent on the effective hydrodynamic lengths, we must conclude that the effective lengths of our fragments, including the 'curved' ones, are very similar under the conditions of our experiments. The rotation time constant for the long kinetoplast DNA is also rather close to those observed for the usual DNA fragments of corresponding length. One way to resolve the conflict of our results with conclusions obtained from other investigations would invoke the assumption that the curved fragments are not 'elastic'. According to this hypothesis, electric field pulses would stretch the curved fragments to an almost straight form and the stretched DNA would return to its equilibrium state with a time constant longer than the rotation time constant.

1. Introduction

Sequence-directed DNA curvature has been under discussion for several years [1] (for reviews, see refs. 2–5). Experimental evidence for sequence-directed curvature has been obtained from the gel migration analysis of a kinetoplast DNA fragment [6–8]. Unusual electrophoretic mobilities were analyzed using kinetoplast DNA fragments [6–9] and synthetic oligonucleotides [10–13]. According to gel migration analysis, $dA_n \cdot dT_n$ blocks with $n \geq 4$ repeated at the helix period induce a clearly detectable DNA curvature [5]. Polyacrylamide gel electrophoresis is by far the most sensitive and convenient method for detecting DNA curvature. However, in the absence of a quantitative theory explaining this migration anomaly, the gel analysis cannot be used to evaluate physical properties of the DNA double helix. Other experimental techniques, such as birefringence [14], electric dichroism [6,15], circularization [16], and electron microscopy [17], were used to demonstrate the existence and to estimate [5] the degree of sequence-directed DNA curvature.

In transient electric birefringence and electric dichroism experiments, DNA molecules are oriented by an electrical field pulse. The transition from the aligned state to random orientation observed after pulse termination can be used to measure the rotational correlation time of the

Dedicated to Professor Manfred Eigen on the occasion of his 60th birthday.

Correspondence address: S. Diekmann or D. Pörschke, Max-Planck-Institut für biophysikalische Chemie, Abteilung biochemische Kinetic, Postfach 2841, Am Fassberg, 3400 Göttingen-Nikolausberg, F.R.G.

molecules. Since the rotational correlation time of a DNA fragment is strongly length dependent [18,19], a curved DNA should display a shorter rotational relaxation time, because its end-to-end distance is smaller [15].

In this paper, we analyze four different DNA fragments of 107 base-pairs (bp) (± 1 bp) length which contain an 80 bp (± 1 bp) long sequence stretch constructed from regular repeats in phase with the helix turn. The sequences of these fragments are listed in table 1. The sequences of three of these fragments (nos. 1, 3 and 4 in table 1) are strongly related to one another [13]. The gel electrophoretic mobility of these 80 bp segments, embedded in longer DNA fragments, has been analyzed extensively [13,20]. Two of these segments (nos. 4 and 5 in table 1) exhibit a strong migration anomaly while the other two migrate normally and serve as controls. In addition, one of these segments (no. 5 in table 1) was used for circularization experiments [16]. The segments showing migration anomaly are supposed to be curved. Since a large part (80 bp) of the 107 bp long fragments is curved, the ratio of the end-to-end distance of the curved to the straight molecules is much smaller than unity. In addition, this length range of DNA fragments is optimal for measurement of the rotational relaxation time [18].

Table 1

Sequences of 'short' DNA fragments used for electro-optical measurements

Capitals denote inserted segments, lower-case letters indicate flanking standard plasmid DNA [32] and lower-case letters in parentheses represent single-stranded ends resulting from cutting by restriction nucleases.

Plasmid (no.)	Insert repeated sequence	Fragment length (bp)	Sequence 5′-*Eco*RI-insert-*Hin*dIII-3′
pK1A108 (1)	GACAGGACTC (10 bp)	107	(aatt)ctcatgtttgacagcttatcatc GACAGGACTC.GACAGGACTC.GACAGGACTC. GACAGGACTC.GACAGGACTC.GACAGGACTC. GACAGGACTC.GACAGGACTCgata(agct)
pK3A108 (3)	GACAAAGCTC (10 bp)	106	(aatt)ctcatgtttgacagcttatcatc GTCAAAGCTC. ACAAAGCTC.GACAAAGCTC. GACAAAGCTC.GACAAAGCTC.GACAAAGCTC. GACAAAGCTC.GACAAAGCTCgata(agct)
pK4A108 (4)	GACAAAACTC (10 bp)	107	(aatt)ctcatgtttgacagcttatcatc GACAAAACTC.GACAAAACTC.GACAAAACTC. GACAAAACTC.GACAAAACTC.GACAAAACTC. GACAAAACTC.GACAAAACTCgata(agct)
pK5/6T217 (5)	ATATATTTTTT AGAGATTTTT (21 bp)	108	(aatt)ctcatgtttgacagcttatcatc GATATATTTTTTAGAGATTTTTATATATTTTTT AGAGATTTTTATATATTTTTTAGAGATTTTTAT ATATTTTTTAGAGACgata(agct)

Thus, a large difference in the rotational relaxation time between curved and straight fragments is expected and should be detectable with high precision. Surprisingly, our electro-optical experiments do not show any large difference in the rotational relaxation times of the four DNA fragments.

2. Materials and methods

The plasmids containing the fragments analyzed here were alkaline extracted and purified by HPLC on Nucleogen 4000 columns (Diagen). After digestion with restriction endonucleases (*Eco*RI and *Hin*dIII, New England Biolabs, Boehringer Mannheim), the DNA fragments were phenol extracted, ethanol precipitated and separated by HPLC on Nucleogen 4000 columns (Diagen). The purity of the fragments was measured by acrylamide gel electrophoresis and ultraviolet spectroscopy. The sequences of all fragments were determined by the sequencing procedure of Maxam and Gilbert [21]. A 419 bp long *Hin*dIII-*Hin*dIII kinetoplast DNA fragment [8] was isolated from a low-percentage acrylamide gel and purified by HPLC. For more details on the cloning procedure of the synthesized oligonucleotides and the preparation of plasmids and DNA fragments, see refs. 8, 13 and 20.

The fragments were dialysed first against several changes of 1 M NaCl, 1 mM sodium cacodylate (pH 7), 0.2 mM EDTA and then extensively against either buffer A containing 1 mM NaCl, 1 mM sodium cacodylate (pH 7), 0.2 mM EDTA or against buffer B containing 1 mM NaCl, 1 mM sodium cacodylate (pH 7) and 100 μM $MgCl_2$.

The electric dichroism was measured using a pulse generator [22] and optical detection system [23,24] described previously. The electric field pulses in the range 2–70 kV/cm were applied to the samples in a cell with 10 mm optical path length and a distance between the Pt electrodes of 5.9 mm. Ultraviolet radiation damage was avoided by the use of an automatic shutter which was opened only for short periods of time synchronized to the field pulses. Both ultraviolet transmission and electric field strength as a function of time were recorded by a Tektronix 7612D transient recorder. The stationary changes of light intensity and electric field strength were evaluated by an interactive procedure supported by graphic routines on an LSI 11/23. The time constants were determined by an efficient deconvolution routine [25] using the facilities of the Gesellschaft für wissenschaftliche Datenverarbeitung, Göttingen mbH.

The DNA fragments, which were analyzed by electric field-jump experiments, were compared to untreated samples on gels of different acrylamide concentrations. Since the analyzed and untreated samples comigrate, there is no indication of any modification of the DNA molecules by the field-jump procedure. In particular, the field-jump procedure does not affect the migration anomaly of 'curved' DNA fragments.

3. Results

3.1. Rotation time constants

Since the dichroism rise curves observed under electric field pulses are strongly influenced by the electric field [26], all the rotation relaxation time constants reported below have been evaluated from dichroism decay curves measured at zero field strength. Nevertheless, the impact of the electric field is strong enough to be clearly reflected in the dichroism decay curves by a dependence of the relaxation response on the electric field strength of the pulse used for orientation. This phenomenon was first described [18] for fragments with more than about 100 bp and was attributed to stretching of the DNA fragments to a straight form by the electric field followed by a reverse 'bending' process after pulse termination. The bending process can be clearly separated from the overall 'tumbling' of the DNA for fragments with more than about 150 bp, but is also existent in the case of shorter fragments. Since the degree of DNA stretching increases with the dipolar forces, the dichroism relaxation observed in the decay curves is dependent upon the electric field strength.

Thus, a field strength dependence of experimental decay time constants should be expected due to a field-dependent contribution from DNA

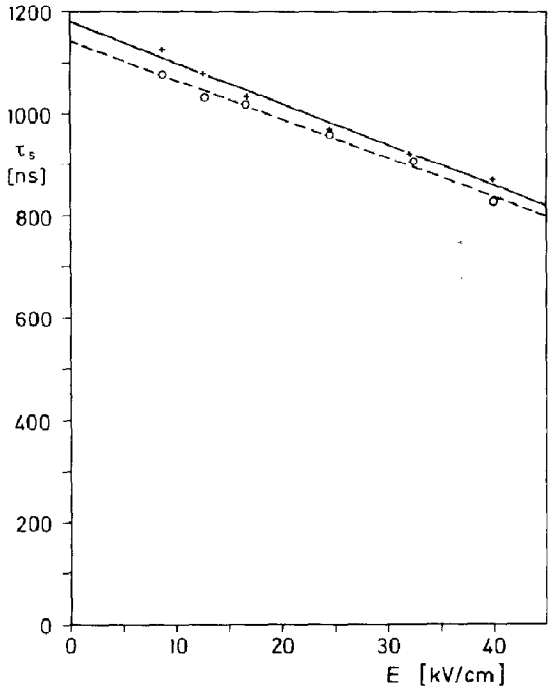

Fig. 1. Rotation correlation time constants τ_s obtained from single-exponential fits of dichroism decay curves as a function of the electric field strength E of the pulse used for orientation for fragments 3 (+) and 5 (○). The straight lines represent linear regressions providing τ_s^0 values at $E = 0$ (buffer A, 20 °C).

bending. A quantitative interpretation of these phenomena is relatively difficult due to the fact that bending of DNA will lead to a distribution of time constants for both bending and overall tumbling.

The fragments studied in the present investigation with 106, 107 and 108 bp (additional four single-stranded residues at each end) are in a range of chain lengths where a contribution due to bending is clearly reflected in the dichroism decay curves after high electric field pulses. However, contributions due to bending are rather small for low field pulses and are not reflected by a clearly separated fast relaxation response [18], but only by a field dependence of time constants, which are evaluated by fits with a single exponential. As shown in fig. 1, the time constant τ_s obtained from single-exponential fits decrease with increasing field strength E. In the range up to 40 kV/cm, τ_s is a linear function of E and thus the value τ_s^0 corresponding to $E = 0$ has been evaluated by linear regression (cf. ref. 27). Similar data have been obtained for all the different fragments in both buffers A and B. The results are compiled in table 2 together with the relative bending amplitude and the bending time constant observed at high field strengths in the range 60–70 kV/cm.

The overall rotation time constants τ_s^0 observed for fragments 1, 3, 4 and 5 are relatively close to each other, although some variation is detected. The decrease of τ_s^0 observed upon addition of 100 μM Mg^{2+} is of similar magnitude to that observed previously for a collection of other fragments [28]. Apart from some minor variation, the magnitude of the τ_s^0 values in both buffers is in the range predicted on the basis of the weakly bending rod model from independent measurements [18,28]. A particularly fast rotational diffusion expected for fragments 4 and 5 is not observed – in spite of their unusual mobility in polyacrylamide gels.

For comparison, the electro-optical parameters of some fragments have also been determined at 2 °C. As shown in table 2, the τ_s^0 values do not increase exactly with the scaling factor η/T as would be expected if the temperature (T) dependence were due exclusively to a change in the water viscosity η. The experimental ratios τ_s^0 (2 °C)/τ_s^0 (20 °C) are 1.70 ± 0.03 and 1.66 ± 0.03 for fragments 3 and 4, respectively, whereas the theoretical factor assuming constant hydrodynamic dimensions is 1.78. Since the deviations are relatively small, these results will not be discussed any further.

The dichroism decay curves observed for the 419 bp long kinctoplast DNA (fragment 'K') had to be fitted by two exponentials at low field strengths ($E \leq 10$ kV/cm), three exponentials at intermediate field strengths and four exponentials in the high-field regime ($E \geq 50$ kV/cm). We have used the slow exponential obtained at low field strengths and applied linear regression (cf. above) for extrapolation to zero field strength. By this procedure we obtained an overall rotation time constant of 14.1 μs at 20 °C in buffer B.

Fragment 5 was also analyzed in the buffer used for gel electrophoresis (45 mM Tris-borate,

Table 2

Parameters obtained from dichroism measurements

τ_s^0, overall rotation correlation time constant; ξ_∞, limit value of the linear dichroism; p, polarizability; E_0, saturation field strength according to the saturating induced dipole model [29] in the square root approximation [30]. Estimated accuracies: τ_s^0 ±2% for fragments 1, 3, 4 and 5, ±5% for fragment 'K', bending amplitudes and time constants ±20%, ξ_∞ ±2%, E_0 ±10%, p ±10%.

Buffer		Temperature						
		20 °C				2 °C		20 °C
	Fragment	1	3	4	5	3	4	K
	Double helix (bp)	107	106	107	108			419
	Single-stranded residues	8	8	8	8			8
A	τ_s^0 (ns)	1050	1170	1070	1140			
	Bending amplitude (%)	17	20	23	29	–	–	
	Bending time (ns)	90	120	120	120			
	ξ_∞	−0.971	−0.988	−0.989	−1.001			
	E_0 (kV/cm)	17.3	16.0	14.6	14.2			
	p (10^{-33} C m^2 V^{-1})	9.96	10.1	7.83	6.87			
B	τ_s^0 (ns)	980	1080	1010	–	1833	1675	14100
	Bending amplitude (%)	17	19	28	–	18	32	
	Bending time (ns)	60	100	120	–	140	170	
	ξ_∞	−1.013	−1.015	−0.990		−1.031	−0.988	
	E_0 (kV/cm)	16.7	16.5	13.6		16.2	13.3	
	p (10^{-33} C m^2 V^{-1})	9.46	9.49	7.24		10.6	7.08	

pH 8.6, 1.25 mM Na-EDTA). The rotational correlation time τ_s^0 found in this buffer was the same as that found in buffer A (within the limits of accuracy, ±2%).

In addition to the overall rotational relaxation time constants, the dichroism decay curves provide values of bending time constants and bending amplitudes for the four 'short' fragments. As shown in table 2, the bending time constants are virtually identical within the limits of accuracy (±20%). Some increase in bending amplitude is observed with increasing curvature of the DNA fragments (cf. section 4). However, the accuracy of these bending amplitudes is limited to ±20% and thus the variation is not much beyond the limit of accuracy.

3.2. Electric dichroism

Some additional information on the structure of the DNA restriction fragments has been obtained by an analysis of the stationary electric dichroism as a function of the electric field strength. The evaluation was based on the saturating induced dipole model [29] using the 'square root' approximation [30]. An example of a set of experimental data and their representation by the model is given in fig. 2. The limit value of the linear dichroism (ξ_∞) corresponding to complete alignment of the fragments, polarizability (p) and the saturation field strength (E_0) are included in table 2.

The ξ_∞ value provides information on the average angle of the transition dipole moments with respect to the long axis of the DNA. A DNA helix in the B form with all the base-pairs aligned perpendicular to the long axis would show a ξ_∞ value of −1.5. The ξ_∞ values obtained for our fragments are around −1.0, which may be explained, for example, by a propeller twist of the base-pairs [31]. The relatively low absolute ξ_∞ values may also be explained – at least partly – by some bending of the DNA helix. However, the dipolar forces induced by the electric field are expected to stretch the DNA fragments to an almost straight form at high electric field strength.

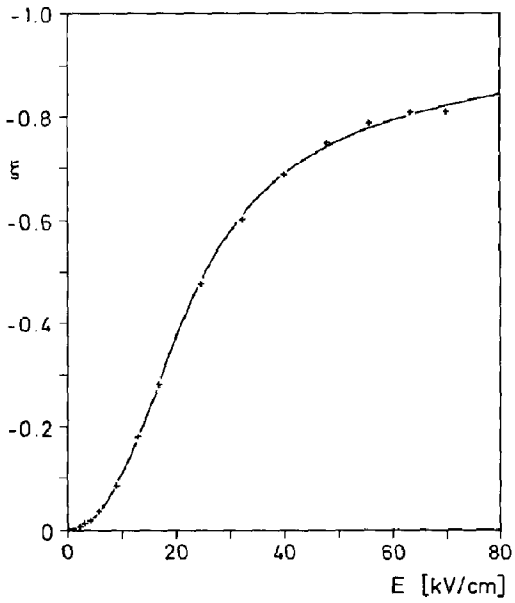

Fig. 2. Stationary values of the reduced linear dichroism ξ as a function of the electric field strength E for fragment 4 in buffer B at 20 °C. (———) Least-squares fit according to the saturating induced dipole model [29] in the square root approximation [30]: limit reduced dichroism $\xi_\infty = -0.990$, polarizability $p = 7.24 \times 10^{-33}$ C m^2 V^{-1}, saturation field strength $E_0 = 13.6$ kV/cm.

According to our results there is virtually no difference in the ξ_∞ value for fragments 1, 3, 4 and 5 and thus the structures should be very similar. Compared to dichroism values obtained for other DNA fragments, the ξ_∞ values found for our present fragments are relatively low, but remain within the range of variations observed previously.

4. Discussion

4.1. DNA fragments containing a kinetoplast curving locus

For a comparison with our present data which have been collected mainly for fragments with insertions constructed by chemical synthesis, we first present a short compilation of some electro-optical data obtained for fragments constructed from kinetoplast DNA.

Recently, Levene et al. [15] determined the rotational relaxation time of two circularly permuted 240 bp long fragments, which contain the curving locus of a kinetoplast DNA fragment. This kinetoplast fragment shows strong gel migration anomaly [6–8]. Both 240 bp long fragments contain the same sequence elements. However, the curving locus has been directed to different positions in the fragment: one close to the center, the other with parts of the curved sequence at both ends of the fragment. The gel mobility is strongly dependent on the relative position of the curving locus in the fragment [7]; fragments having the curved sequence in the middle show much stronger gel migration anomaly. According to measurements of the electric dichroism by Levene et al. [15], the two 240 bp fragments show a difference of 20% in their rotational relaxation times. From hydrodynamic theory the authors [15] calculate a curving angle of 84° for the curved sequence embedded in these fragments.

Hagerman [14] developed a differential transient birefringence technique which was used to measure the difference between a strongly curved DNA fragment of 242 bp length and a DNA fragment of equal length with normal gel mobility. The 242 bp curved fragment is a palindromic dimer of a 121 bp sequence which contains the curving locus of the same kinetoplast DNA fragment [6–8]. Since the palindromic fragment contains two copies of the curving locus analyzed by Levene et al. [15], a particularly fast rotation diffusion may be expected for this fragment. However, the difference with respect to the reference DNA determined by Hagerman is only up to 24%.

In addition, Marini et al. [6] and Hagerman [14] measured the rotational relaxation time of the whole 410 bp long kinetoplast DNA fragment (*Sau*3A ends). While Marini et al. [6] apparently missed the slow phase of the decay process entirely [14], Hagerman [14] measured a slow rotational relaxation process with a time constant of 23.1 μs for this 410 bp fragment (at 3°C in sodium phosphate buffer). We have analyzed a fragment of the same sequence with a few additional framing base-pairs (419 bp total length, *Hin*dIII-*Hin*dIII [8]), which also shows a strong anomaly of gel migration. Our measurements per-

formed at 20°C in a buffer containing 100 μM Mg^{2+} (buffer B) provided a time constant of 14.1 μs for the slowest component of rotational diffusion. A correction for the temperature difference (1.77×14.1 μs = 25 μs) shows that our rotation time constant is rather close to that reported by Hagerman. Comparison with dichroism decay time constants obtained by Diekmann et al. [18] shows that the rotation time of the anomalous kinetoplast DNA is very similar to those of standard DNA fragments with usual gel mobility.

4.2. DNA fragments with constructed insertions

For a more detailed analysis of electro-optical parameters we constructed and analyzed shorter DNA fragments of 107 bp (±1 bp) length. In this range of chain lengths the rotational diffusion is dominated by a single relaxation process [18] and thus the relaxation time constant can be determined to a higher accuracy.

Our fragments contain a central block of repeated sequences framed by short segments of standard plasmid DNA (cf. table 1). The numbers given to these fragments reflect the number of adjacent dA residues in the repeated part of the sequence. The repeated part of fragments 1, 3 and 4 contains a central block of four purines with the sequences dAGGA, dAAAG and dAAAA, respectively. The repeating sequence of fragment 5 has 21 bp with blocks of five and six dT residues and an average repeat distance for the dT blocks of 10.5 bp. The gel mobility of these sequences embedded in longer DNA fragments has been studied extensively [13,16,20]. Two of these *Hae*III fragments (nos. 1 and 3) show no (no. 1) or hardly any (no. 3) gel migration anomaly and serve as control molecules for the other two fragments which show a strong anomaly. All four molecules contain the same 5′ and 3′ sequences framing the insertion sequences. Since at least one of these constructions shows no anomaly, neither the framing sequences nor the insertion of 80 bp at the *Cla*I site per se can be the origin of the anomaly. In addition, the framing sequences alone without the insertion also show no migration anomaly [8].

The insertions containing $dA_n \cdot dT_n$ blocks with $n \geq 4$ (fragments 4 and 5) induce gel migration anomalies for all fragments embedding these sequences. Both fragments (nos. 4 and 5) show strong anomalies with different temperature and salt dependence [20]. The gel migration anomalies of *Eco*RI-*Hin*dIII fragments 3 and 4 (see table 1) have been measured as dimers [20]. Since the anomalies of short curved DNA fragments are relatively small [8], the mobilities of the short fragments listed in table 1 were determined in 10% acrylamide gels but were not analyzed in further detail. The apparent lengths relative to the sequence lengths (k factor [8,13,20]) are 1.02, 1.05, 1.26 and 1.38 (±0.02) for fragments 1, 3, 4 and 5, respectively.

4.3. Estimates of the degree of curvature

The curvature of DNA fragments may be estimated by enzymatic ligation of the fragments and analysis of the product distribution: the extent of circle formation and the chain length distribution of the circles provide information on the degree of curvature.

Ulanovsky et al. [16] measured the probability of circle formation for double-helical segments with 21 bp ligated to tandem multimers. Oligomer helices of the same sequence were used to construct the insertion of fragment 5 (cf. ref. 20 and table 1). Thus, the results of these circularization experiments can be used to estimate the degree of curvature of the insertion sequence of fragment 5. Ulanovsky et al. [16] found a circularization maximum at 137 bp. When the curvature is addressed to the length of the repetitive sequence without counting the 5′ flanking 23 bp normal DNA derived from pBR322 (see ref. 32), we estimate a curvature of about 208° for the 79 bp insertion of fragment 5 (the first G : C and last C : G base-pair not included). When the 23 bp normal DNA is assumed to be straight, the end-to-end distance of this fragment is approximately half its contour length.

For the 80 bp insertion sequence constructed from repeated dA_4 blocks (fragment 4) we calculate a curvature of 144°, when a deflection angle of 18° per dA_n block (two junctions) is assumed [15]. Using the results of the circularization experiment [16] and addressing the curvature to dAA

dinucleotides, we estimate a curvature of 152°. When addressing the curvature to the number of $dA_n \cdot dT_n$ blocks with $n \geq 4$ and using the same data [16], we obtain a curvature of 220°. Depending on the procedure, an end-to-end distance of less than 0.7 relative to the helix length is obtained for fragment 4.

As a simple visual aid, the approximate shape of fragment 5 is presented in fig. 3, using the curvature evaluated from circularization experiments. Obviously, the effective hydrodynamic dimensions of this object are strongly reduced compared to a piece of straight DNA with the same number of base-pairs. Since the rotation time constant of the curved DNA shown in fig. 3a has not yet been calculated, for comparison we show a molecule with the same contour length which is bent at its center with an angle of 30° between the two arms (fig. 3b). The electro-optical decay process for the bent rod shown in fig. 3b has been calculated by Mellado and Garcia de la Torre [33] relative to a straight rod of the same length. In this case bending leads to a reduction of the calculated effective rotation time constant by approx. 76%! Although the shapes of the objects shown in fig. 3a and b are not equivalent, the comparison should be useful for demonstrating that a molecule with stable curvature as shown in fig. 3a should be associated with a much lower rotation time constant than that of a straight molecule of the same length.

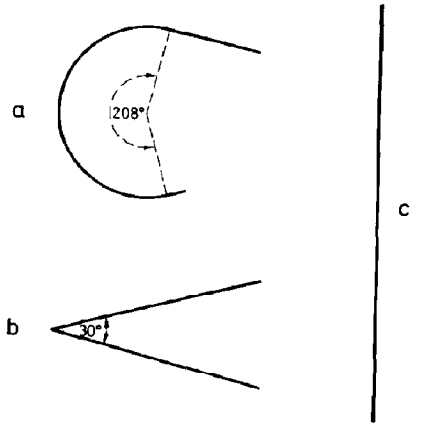

Fig. 3. Sketch of different shapes of a DNA fragment: (a) 79 bp with curvature corresponding to 208° with 23 and 4 bp straight DNA at the ends, respectively; (b) DNA of same contour length with bend of 30° at its center; (c) straight DNA of same contour length.

4.4. Structure of curved DNA fragments easily distorted?

Although the results obtained from circularization and gel migration experiments indicate strong curvature for fragments 4 and 5, we do not find any evidence for strong curvature from the rotation relaxation time constants. The contrast between these different results can hardly be resolved. As mentioned above, data obtained from gel mobility experiments cannot be evaluated quantitatively, because a complete theory of gel mobility is not available. However, it is hardly possible to argue against the circularization experiments. Thus, we should examine our electro-optical experiments for possible artefacts. It has been established that high electric field pulses may cause special reactions of DNA double helices: for example, a transition to single strands [34], an association reaction driven by dipole interactions [35] and stretching of bent DNA helices [18,28]. All these special reactions have been analyzed quantitatively and the conditions for their occurrence have been defined exactly. According to this information, none of the known field-induced reactions has any influence on the rotation time constants τ_s^0 given in table 2. As a particular precaution we have measured our rotation time constants as a function of the electric field strength down to very low values and also extrapolated to zero field strength. Using the same procedure it had been possible to detect the small length increase induced by the intercalation of a single ethidium molecule per DNA double helix of 95 bp, and also the bending of specific DNA fragments by binding of cyclic AMP receptor in the presence of cyclic AMP (cf. refs. 27 and 36). Due to the contrast between the results obtained for curved DNA fragments by the different methods, we are compelled to seek other extraordinary effects which could influence our electro-optical results. One possibility of resolving the contrast appears to be particularly interesting and thus

should be mentioned. As already discussed above, the dipolar forces induced by the electric field induce not only orientation but also stretching of bent helices. This effect has been observed at high electric field strengths and has also been interpreted quantitatively [28]. The stretching effect appears to be rather small at low field strengths. Nevertheless, strongly curved DNA fragments may be particularly sensitive to field-induced stretching and thus may already be stretched at low field strengths. Usually, stretched DNA fragments show elastic properties and return quickly to their bent form after pulse termination [18,28]. In these cases the slow rotation time constant reflects the effective hydrodynamic length at equilibrium. However, the possibility cannot be ruled out that some DNA sequences are 'not elastic' – in the sense that a stretched form does not return quickly to its curved equilibrium form. Of course, 'quickly' is a relative term and should be specified more exactly. In our case, the reference is the overall rotational relaxation time constant τ_s^0. If the curving time constant τ_c is large compared to τ_s^0, τ_s^0 is measured for the stretched form of the fragment and does not reflect the effective hydrodynamic length at equilibrium.

Although we do not have any direct evidence for such 'inelastic' properties of our DNA fragments, a molecular interpretation in terms of a junction model of standard B-DNA with another form of DNA appears to be attractive. One of the models to explain DNA curvature assumes that the $dA_n \cdot dT_n$ blocks form a B′-form DNA structure [13,37,38], while the sequences in between are in standard B form. We may explain our present data by the assumption that electric field pulses turn DNA segments with unusual structure into B-DNA and thus convert curved to straight DNA. If the back-reaction after pulse termination is slow (relative to τ_s^0 corresponding to a few microseconds), the statistical distribution of the fragment by rotational Brownian motion is complete before the $dA_n \cdot dT_n$ blocks have formed their native conformation. Since the model requires that curved DNA is already stretched almost completely at low electric fields around 2 kV/cm, the model also implies that the free energy for curving of our DNA fragments is relatively small. This is in agreement with observations from band shift experiments [8], which suggest the interpretation that the structure of curved DNA can be easily distorted. Although the model is still speculative, it may be useful as a focus for the design of further experiments.

Acknowledgements

The expert technical assistance of J. Ronnenberg and B. Preitz is gratefully acknowledged. S.D. wishes to thank Dr. M. Kahlweit and the Deutsche Forschungsgemeinschaft (grant Di 258/3-1) for support.

References

1 E.N. Trifonov and J.L. Sussman, Proc. Natl. Acad. Sci. U.S.A. 77 (1980) 3816.
2 E.N. Trifonov, CRC Crit. Rev. Biochem. 19 (1985) 89.
3 J. Widom, BioEssays 2 (1985) 11.
4 D.M. Lilley, Nature 320 (1986) 487.
5 S. Diekmann, in: Nucleic acids and molecular biology, eds. F. Eckstein and D.M. Lilley, vol. 1 (Springer, Berlin, 1987) in the press.
6 J.C. Marini, S.D. Levene, D.M. Crothers and P.T. Englund, Proc. Natl. Acad. Sci. U.S.A. 79 (1982) 7664; Correction: J.C. Marini and P.T. Englund, Proc. Natl. Acad. Sci. U.S.A. 80 (1983) 7678.
7 H.M. Wu and D.M. Crothers, Nature 308 (1984) 509.
8 S. Diekmann and J.C. Wang, J. Mol. Biol. 186 (1985) 1.
9 P.A. Kitchin, N.A. Klein, K.A. Ryan, K.L. Gann, C.A. Rauch, D.S. Kang, R.D. Wells and P.T. Englund, J. Biol. Chem. 261 (1986) 11302.
10 P.J. Hagerman, Biochemistry 24 (1985) 7033.
11 P.J. Hagerman, Nature 321 (1986) 449.
12 H.S. Koo, H.M. Wu and D.M. Crothers, Nature 320 (1986) 501.
13 S. Diekmann, FEBS Lett. 195 (1986) 53.
14 P.J. Hagerman, Proc. Natl. Acad. Sci. U.S.A. 81 (1984) 4632.
15 S.D. Levene, H.M. Wu and D.M. Crothers, Biochemistry 25 (1986) 3988.
16 L. Ulanovsky, M. Bodner, E.N. Trifonov and M. Choder, Proc. Natl. Acad. Sci. U.S.A. 83 (1986) 862.
17 J. Griffith, M. Bleyman, C.A. Rauch, P.A. Kitchin and P.T. Englund, Cell 46 (1986) 717.
18 S. Diekmann, W. Hillen, B. Morgeneyer, R.D. Wells and D. Pörschke, Biophys. Chem. 15 (1982) 263.
19 P.J. Hagerman, Biopolymers 20 (1981) 1503.
20 S. Diekmann, Nucleic Acids Res. 15 (1987) 247.

21 A.M. Maxam and W. Gilbert, Methods Enzymol. 65 (1980) 499.
22 H.H. Grünhagen, Messtechnik (1984) 19.
23 D. Pörschke, Nucleic Acids Res. 8 (1980) 1591.
24 C.R. Rabl, Thesis, Universitat Konstanz (1984).
25 D. Pörschke and M. Jung, J. Biomol. Struct. Dyn. 2 (1985) 1173.
26 D. Pörschke, Biophys. Chem. 22 (1985) 237.
27 D. Pörschke, W. Hillen and M. Takahashi, EMBO J. 3 (1984) 2873.
28 D. Pörschke, J. Biomol. Struct. Dyn. 4 (1986) 373.
29 S. Diekmann, W. Hillen, M. Jung, R.D. Wells and D. Pörschke, Biophys. Chem. 15 (1982) 157.
30 S. Diekmann, M. Jung and M. Teubner, J. Chem. Phys. 80 (1984) 1259.
31 M. Hogan, N. Dattagupta and D.M. Crothers, Proc. Natl. Acad. Sci. U.S.A. 75 (1978) 195.
32 J.G. Sutcliffe, Cold Spring Harbor Symp. Quant. Biol. 43 (1979) 77.
33 P. Mellado and J. Garcia de la Torre, Biopolymers 21 (1982) 1857.
34 S. Diekmann and D. Pörschke, Biophys. Chem. 16 (1982) 261.
35 D. Pörschke, H.J. Meier and J. Ronnenberg, Biophys. Chem. 20 (1984) 225.
36 D. Pörschke, N. Geisler and W. Hillen, Nucl. Acids Res. 10 (1982) 3791.
37 S. Arnott, R. Chandrasekaran, I.H. Hall and L.C. Puigjaner, Nucleic Acids Res. 11 (1983) 4141.
38 E. von Kitzing and S. Diekmann, Eur. Biophys. J. (1987) in the press.